JACS
JOURNAL OF THE AMERICAN CHEMICAL SOCIETY
Article
pubs.acs.org/JACS

Ultrafast (1 μs) Mixing and Fast Protein Folding in Nanodrops Monitored by Mass Spectrometry

Daniel N. Mortensen and Evan R. Williams*

Department of Chemistry, University of California, Berkeley, California 94720-1460, United States

Supporting Information

ABSTRACT: The use of theta-glass emitters and mass spectrometry to monitor reactions that occur as fast as one μs is demonstrated. Acidified aqueous solutions containing unfolded proteins are mixed with aqueous ammonium acetate solutions to increase the solution pH and induce protein folding during nanoelectrospray ionization. Protein charge-state distributions show the extent to which folding occurs, and reaction times are obtained from known protein folding time constants. Shorter reaction times are obtained by decreasing the solution flow rate, and reaction times between 1.0 and 22 μs are obtained using flow rates between 48 and 2880 pL/s, respectively. Remarkably similar reaction times are obtained for three different proteins (Trp-cage, myoglobin, and cytochrome *c*) with folding time constants that differ by more than an order of magnitude (4.1, 7, and 57 μs, respectively), indicating that the reaction times obtained using rapid mixing from theta-glass emitters are independent of protein identity. A folding time constant of 2.2 μs is obtained for the formation of a β-hairpin structure of renin substrate tetradecapeptide, which is the fastest folding event measured using a rapid mixing technique. The 1.0 μs reaction time obtained here is about an order of magnitude lower than the shortest reaction time probed using a conventional mixer (8 μs). Moreover, this fast reaction time is obtained with a 48 pL/s flow rate, which is 2000-times less than the flow rate required to obtained the 8 μs reaction time using a conventional mixer. These results indicate that rapid mixing with theta-glass emitters can be used to access significantly faster reaction times while consuming substantially less sample than in conventional mixing apparatus.

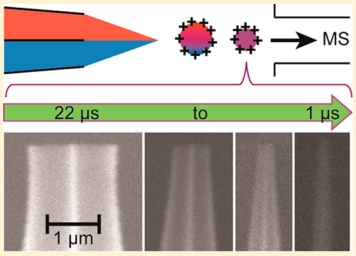

INTRODUCTION

Information about reaction kinetics, including protein folding[1−3] and unfolding,[4] is often obtained by rapidly mixing two or more solutions. Conventional mixing devices include chaotic,[5] turbulent,[6] and laminar[2,3] flow mixers. Shorter reaction times are often obtained by increasing the solution flow rate. The shortest reaction time achieved with a conventional mixer is 8 μs using a laminar flow mixer with a ∼100 nL/s flow rate.[2] This mixing time is insufficient to observe some fast protein folding events, such as the folding of the 20 residue "mini-protein" Trp-cage, which has a folding time constant of 4.1 μs.[7] Mass spectrometry (MS) is an excellent detector for measuring reaction products resulting from rapid mixing experiments owing to its high sensitivity, high chemical specificity, and rapid speed of analysis.[8] Several different in-line mixers have been coupled with MS including stopped,[1] continuous,[4,9] and laminar[2,3] flow devices. The shortest reaction time achieved using a conventional mixer coupled with MS is 200 μs with a laminar flow mixer and a 10 μL/s flow rate.[3]

Solutions can be mixed prior to MS during electrospray ionization (ESI), which has been done using multiple channel electrospray,[10,11] fused-droplet electrospray,[12] extractive electrospray,[13,14] and dual-sprayer microchips.[15,16] Solution-phase reactions have also been carried out in charged microdroplets and monitored with MS using desorption electrospray ionization,[17,18] ambient ion soft landing,[19] and microdroplet fusion, which is accomplished by orthogonally colliding ESI droplets.[20] Microdroplet fusion MS has been used to measure bimolecular reduction−oxidation, protein unfolding, and hydrogen/deuterium exchange at reaction times of >13 μs.[20] This reaction time was obtained from the droplet velocity and the distance between the droplet collision point and the entrance to the mass spectrometer. Mixing times in these experiments were estimated to be less than a few microseconds.

Recently, theta-glass emitters (double-barrel wire-in-a-capillary emitters that resemble the Greek letter θ "theta" when turned on end) have been used to mix solutions during the ESI process. Mixing with theta-glass emitters likely occurs in a few microseconds or less[21] and has been used to measure noncovalent complexation,[21,22] hydrogen/deuterium exchange,[22] bimolecular reduction−oxidation,[21] protein folding[23] and unfolding,[23,24] and to introduce supercharging reagents to protein solutions during ESI.[24]

The lifetime of the droplets formed using the theta-glass emitters controls the extent to which solution-phase reactions can occur in these droplets.[21,23] The ESI droplet lifetime depends on several factors including the solution composition[23,25] and the initial droplet diameter.[25] The initial droplet diameter can be varied by changing the solution flow rate,[26−29] which depends on both the inner diameters of the electrospray emitter tips and the backing pressure applied to the solutions inside the emitters.[29,30] Reaction times between 7 and 25 μs, depending on solution composition, have been obtained for droplets formed from theta-

Received: December 14, 2015
Published: February 22, 2016

DOI: 10.1021/jacs.5b13081
J. Am. Chem. Soc. 2016, 138, 3453−3460

glass emitters operating at a flow rate of ~1 nL/s.[23] These reaction times were obtained from the extent of protein folding that occurs during nanoESI and known protein folding time constants obtained in bulk solution. Information about the conformation of proteins in solution is obtained from the charge-state distributions of the protein ions formed by ESI. Folded globular conformers are less highly charged than unfolded conformers,[31−34] and the relative abundances of different protein conformers can be obtained by modeling the bimodal or multimodal charge-state distributions.[34,35] The short reaction times obtained using rapid mixing from theta-glass emitters indicate that this technique can be used to access fast reaction times while consuming substantially less sample than is used in conventional mixing apparatus. However, methods for varying the reaction time at short time scales using rapid mixing from theta-glass emitters have not previously been demonstrated.

Here, theta-glass emitters are used to mix acidified aqueous solutions containing a protein with aqueous ammonium acetate to increase the solution pH and induce protein folding during nanoESI. The extent of protein folding that occurs in these experiments is controlled by varying the solution flow rate, and reaction times between 1.0 μs at 48 pL/s and 22 μs at 2880 pL/s are obtained from the extent of folding that occurs in these experiments and known folding time constants of different proteins. The 1.0 μs reaction time is significantly less than the 8 μs reaction time reported for a conventional mixer.[2] The 1.0 μs reaction time is obtained using a flow rate (48 pL/s) that is 2000-fold less than that required to obtained the 8 μs reaction time using a conventional mixer (~100 nL/s). Results from this study demonstrate that ultrafast (1 μs) protein folding reactions can be readily investigated using rapid mixing from theta-glass emitters coupled with MS and that substantially less sample is required compared to conventional mixing apparatus. This method should enable a wide range of fast reactions to be measured including complex reactions with multiple reaction products.

EXPERIMENTAL SECTION

Mass spectra are acquired using a 9.4 T Fourier-transform ion cyclotron resonance mass spectrometer that is described elsewhere.[36] Rapid mixing is performed using theta-glass capillaries (Warner Instruments, LLC; Hamden, CT) that have tips that are pulled using a model p-87 Flaming/Brown micropipette puller (Sutter Instruments Co.; Novato, CA). The tips of the capillaries are imaged on carbon tape at 10 000-times magnification using a TM-1000 scanning electron microscope (Hitachi High-Technologies Co.; Tokyo, Japan). Grounded platinum wires are inserted into the capillaries so as to contact the solutions in each barrel, and a backing pressure is applied to the back end of the capillaries. NanoESI is initiated by applying a potential of about −700 V to the heated capillary of the ESI interface. Data are acquired using a Predator data station,[37] and mass spectra are background subtracted. To determine flow rates, the theta-glass emitters are weighed before and after electrospraying for a fixed time using an A-200DS analytical balance (Denver Instrument Company, Bohemia, NY) with a lower mass range of 0.01 mg and a reproducibility (standard deviation) of 0.02 mg. Temperature-dependent studies are conducted using single-barrel wire-in-a-capillary electrospray emitters prepared by pulling borosilicate capillaries (Warner Instruments) into 1.83 ± 0.04 μm o.d. tips. A NiCr wire is wrapped around a cylindrical aluminum jacket that holds the capillaries and is used to resistively heat the capillaries during nanoESI. The temperature of the aluminum jacket is measured using a thermocouple (Omega, Stanford, CT). This device is described elsewhere.[34] Traveling wave ion mobility spectrometry drift times in nitrogen gas are measured using a Synapt G2-Si High Definition Mass Spectrometer (Waters, Milford, MA, USA) with a wave velocity of 500 m/s, a wave height of 40 V, and helium and nitrogen flow rates of 180 and 90 mL/s, respectively.

Average charge states are computed as abundance weighted sums of the individual charge states. All uncertainties reported are standard deviations determined from triplicate measurements. The initial pH values of droplets formed upon rapid mixing of two solutions from the theta-glass emitters are estimated to be within ±0.2 of the pH of those solutions mixed at a 1:1 ratio. This estimate is determined using the initial concentrations of acetic acid ($pK_a = 4.8$) and ammonia ($pK_b = 4.8$, both at 25 °C)[38] in the droplets. Initial droplet concentrations are determined from the initial concentrations of the solutions in each barrel and the relative flow rates of these solutions during nanoESI. Relative flow rates are monitored using Leu- and Met-enkephalin as internal standards as described previously.[21]

Ammonium acetate, 18-crown-6, Leu- and Met-enkephalin acetate salt hydrates, equine apo-myoglobin and cytochrome *c*, and renin substrate tetradecapeptide are obtained from Sigma-Aldrich (St. Louis, MO), glacial acetic acid and NaCl from Fisher Scientific (Fair Lawn, NJ), KCl from Mallinckrodt Baker, Inc. (Phillipsburg, NJ), and Trp-cage from AnaSpec Inc. (Fremont, CA).

RESULTS AND DISCUSSION

Controlling Solution Flow Rates. The solution flow rates in the theta-glass emitters can be varied by changing the backing pressure applied to the solutions in the emitters and by making emitters with tips that have different outer diameters (o.d.).[29,30] Smaller initial droplet sizes are formed with lower solution flow rates[29] and with smaller tip sizes.[39] The effect of the backing pressure on the flow rate was investigated by varying the pressure between 5 and 40 psi using theta-glass emitters with ~1465 nm o.d. tips. Flow rates are obtained by spraying an aqueous solution of 500 μm 18C6 and 500 μm NaCl until the mass of the solution in the tip decreases by at least 0.5 mg and by measuring the change of mass with time (between ~10 min and ~2 h, depending on the flow rate). These measurements show that the flow rate increases linearly with increasing backing pressure from 383 pL/s at 5 psi to 2880 pL/s at 40 psi (Figure 1a).

The effect of the size of the o.d. of the tips of the theta-glass emitters on the flow rate was investigated by varying the o.d. of the tips between 244 ± 61 and 1465 ± 134 nm and using a 10 psi backing pressure. Electron micrographs of the various size tips are provided in the Supporting Information (Figure S1). The flow rate increases linearly with increasing tip o.d., from 48 pL/s

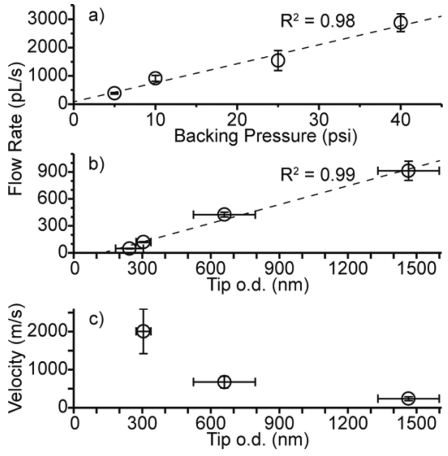

Figure 1. Solution flow rates as a function of (a) the backing pressure applied to the solutions during nanoESI using theta-glass emitters with ~1465 nm o.d. tips and (b) the o.d. of the tips of the theta-glass emitters using a 10 psi backing pressure. Dashed lines are linear fits to the data. (c) Solution velocities at the tips of the theta-glass emitters as a function of the tip o.d.

DOI: 10.1021/jacs.5b13081
J. Am. Chem. Soc. 2016, 138, 3453−3460

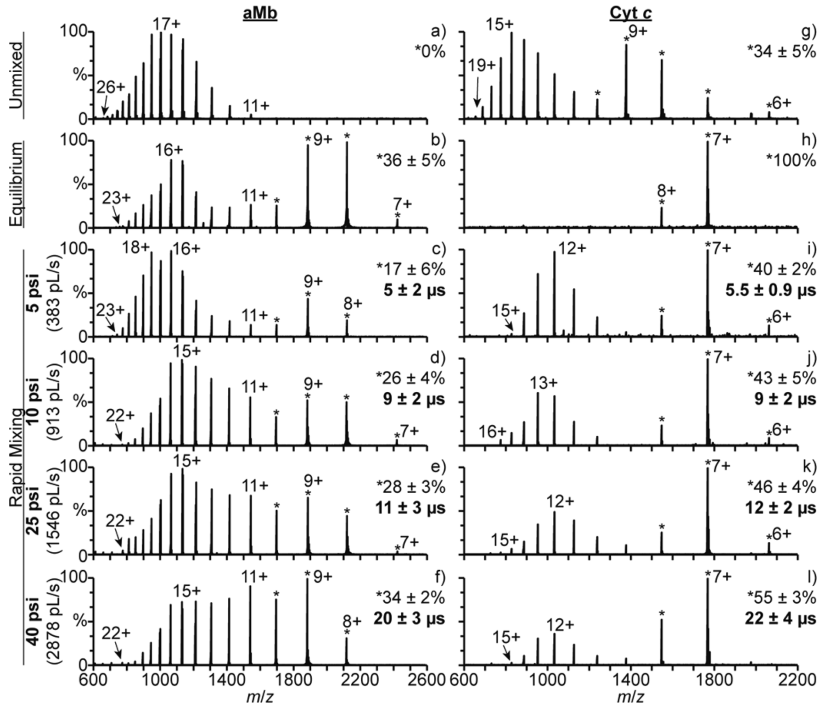

Figure 2. Mass spectra of (a) an acidified aqueous aMb solution (pH = 2.9), (b) the acidified aMb solution mixed with a 100 mM aqueous ammonium acetate solution at a 1:1 ratio prior to nanoESI (equilibrium; pH = 4.7), the acidified aMb solution mixed with the ammonium acetate solution using the theta-glass emitters and backing pressures of (c) 5, (d) 10, (e) 25, and (f) 40 psi, (g) an acidified aqueous cyt *c* solution (pH = 2.8), (h) the acidified cyt *c* solution mixed with the ammonium acetate solution at a 1:1 ratio prior to nanoESI (equilibrium; pH = 4.4), and the acidified cyt *c* solution mixed with the ammonium acetate solution using the theta-glass emitters and backing pressures of (i) 5, (j) 10, (k) 25, and (l) 40 psi. Inset percentages are the relative abundances of the charge states corresponding to folded protein conformers (denoted with ∗).

at ∼244 nm to 913 pL/s at ∼1465 nm (Figure 1b) even though the cross-sectional area of the tips increases quadratically with the tip diameter. The linear relationship between tip size and flow rate is consistent with results reported for single-barrel emitters with tip o.d.s of between 1 and 5 μm.[30] The relationship between flow rate and cross-sectional area of the tip indicates that the velocity of the solution exiting an emitter changes with tip size. The velocity of a solution as it exits the emitter was obtained by dividing the solution flow rate by the emitter tip orifice area. The latter value was estimated as an ellipse with diameters equal to the i.d. of the tips perpendicular to and parallel to the inner divider less the area occupied by the inner divider. Solution velocities were not estimated for the smallest (∼244 nm o.d.) tips because the i.d. and central divider were not resolvable. The velocity of the solution at the tip of the theta-glass emitters as a function of the tip o.d. is shown in Figure 1, panel c. The solution velocity increases significantly with decreasing tip size. The electric field at the tip of the emitter also increases with decreasing tip size, and this may play a role in the increasing velocity with decreasing tip size.

To determine whether complete mixing between the solutions in the two channels of the theta-glass emitters occurs during nanoESI, a solution containing 18-crown-6 (18C6) was mixed with a solution containing KCl, and the rapid equilibration complexation reaction between 18C6 and K^+ was measured. The extent of complexation reaction that occurs in these experiments is obtained from the abundance of the complex $[18C6 + K]^+$ relative to that of the complex $[18C6 + Na]^+$ as described previously[21] (Supporting Information, Figure S2). This reaction reaches equilibrium during nanoESI at each flow rate, indicating that the solutions loaded into the different barrels of the theta-glass emitters mix completely in these experiments.

Reaction Times and Backing Pressure. To determine the reaction times that are accessible with these theta-glass emitters, the folding of proteins with known folding rate constants was investigated. In aqueous solution, apo-myoglobin (aMb) is unfolded below pH = 3, has a partially unfolded globular structure at pH = 4, and has a compact globular structure similar to that of native holo-myoglobin between pH = 5 and 7.[40] NanoESI of an acidified aqueous aMb solution (pH = 2.9) results in the production of the 11−26+ charge states (Figure 2a), consistent with this protein adopting unfolded conformations in this solution. Results from mixing this acidified aMb solution with a 100 mM aqueous ammonium acetate solution at a 1:1 ratio prior to nanoESI (equilibrium; pH = 4.7) are shown in Figure 2, panel b. The charge-state distribution is bimodal, and the high charge state distribution corresponding to unfolded structures is shifted to slightly lower charge. The 7−10+ charge states correspond to folded conformers and constitute 36 ± 5% of aMb. The 11+ charge state is more abundant than the 10+ and 12+ charge states, suggesting that a partially folded, perhaps intermediate conformer, may also be present.

The effects of the solution flow rate on the extent of folding that occurs during nanoESI were determined by mixing the acidified aMb solution with the ammonium acetate solution using the theta-glass emitters with backing pressures of between 5 and 40 psi (Figure 2c−f, in order of increasing backing pressure). The same charge states are observed as those measured when these solutions are at equilibrium (Figure 2b), but the relative abundance of the folded fraction of aMb (7−10+) increases with backing pressure from 17 ± 6% at 5 psi to 34 ± 2% at 40 psi. These results indicate that the extent of folding that occurs during the nanoESI process increases with increasing backing pressure. Interestingly, the relative abundance of the 11+

DOI: 10.1021/jacs.5b13081
J. Am. Chem. Soc. 2016, 138, 3453−3460

charge state also increases with increasing backing pressure, consistent with this charge state corresponding to a short-lived folding intermediate. The reaction time upon rapid mixing using the theta-glass emitters can be obtained from the extent of protein folding that occurs by modeling this as a two-state folding reaction.[41] The integrated rate law for a two-state folding reaction is

$$t = \tau \ln\left(\frac{A_e - A_o}{A_e - A_t}\right) \quad (1)$$

where t is time, τ is the protein folding time constant, and A_e, A_o, and A_t are the relative abundances of the folded protein conformer at equilibrium and at times 0 and t, respectively. The initial collapse of unfolded aMb to a globular conformer occurs with a 7 μs time constant,[42] and the formation of a conformer similar to that of native holo-myoglobin occurs in greater than 1 ms.[43] Previous results using theta-glass emitters with ~1 nL/s flow rates indicated a 9 μs reaction time.[23] Thus, only the initial collapse of aMb is likely to occur to a significant extent in the droplets formed here.

To determine the extent to which the folded structures from the equilibrium and rapid mixing experiments are similar, drift times of the corresponding charge states (8−10+) are obtained using traveling wave ion mobility spectrometry (TWIMS). Drift times obtained for the 8−10+ charge states of aMb resulting from the rapid mixing experiments are between 1 and 3% longer than those obtained for the same charge states resulting from the equilibrium experiments (Supporting Information, Figure S3a−c). These results suggest that the 8−10+ charge states resulting from the rapid mixing experiments correspond to slightly less compact structures than those resulting from the equilibrium experiments, consistent with the initial collapse expected on this fast time scale.

The reaction times in these rapid mixing experiments are obtained from the relative abundances of the folded fraction of aMb obtained in the unmixed, equilibrium, and rapid mixing experiments and the 7 μs time constant of the initial collapse of aMb using eq 1. These reaction times are indicated on the corresponding mass spectra (Figure 2c−f). The reaction time increases with increasing backing pressure from 5 ± 2 μs at 5 psi to 20 ± 3 μs at 40 psi.

To determine the accuracy of these reaction times, another protein with a significantly different folding time constant was investigated. In aqueous solution, cytochrome c (cyt c) adopts a native folded conformer between pH = 3 and 7 and is unfolded at pH = 2.[44,45] Cyt c also adopts a globular "A" state at salt concentrations of ≥0.2 M,[46] and a partially folded intermediate may form in solutions with lower salt concentrations.[47,48] NanoESI of an aqueous cyt c solution at pH = 2.8 results in a bimodal charge-state distribution (Figure 2g), indicating that both folded (6−10+) and unfolded (11−19+) conformers exist in solution at this pH and that the folded form comprises 34 ± 5% of the population. Results from mixing this acidified cyt c solution with a 100 mM aqueous ammonium acetate solution at a 1:1 ratio prior to nanoESI (equilibrium; pH = 4.4) are shown in Figure 2, panel h. Only the 7+ and 8+ charge states are observed, indicating that cyt c is predominantly folded in this solution. The slightly lower charging of the folded form resulting from this solution (Figure 2h) compared to that from the unmixed cyt c solution (Figure 2g) may be a result of the different solution composition or of changes to the structure of the folded conformer. The mixed solution has a higher ionic strength and thus may result in more compact conformers. Results from mixing the acidified cyt c solution with the ammonium acetate solution using the theta-glass emitters with backing pressures of between 5 and 40 psi are shown in Figure 2, panels i−l in order of increasing backing pressure. There are charge states corresponding to both folded (6−8+) and unfolded (9−16+) structures in each spectrum, and the relative abundance of the folded form increases with backing pressure from 40 ± 2% at 5 psi to 55 ± 3% at 40 psi.

The initial folding of cyt c occurs with a 57 μs time constant,[44] and other folding steps may occur with time constants of ≥600 μs.[48−50] The TWIMS ion mobility drift times for the 6−8+ charge states of cyt c formed in the rapid mixing and equilibrium experiments are indistinguishable (Supporting Information, Figure S3d−f). This result indicates that any differences in structure are indistinguishable based on the collisional cross-section alone. On the basis of the 5−20 μs reaction times obtained here for aMb, only the initial folding step of cyt c is likely to occur to a significant extent in these experiments. Thus, only the 57 μs time constant for the initial folding step of cyt c is considered in obtaining the reaction times for these experiments, which are indicated on the respective mass spectra (Figure 2i−l). The reaction time increases with backing pressure from 5.5 ± 0.9 μs at 5 psi to 22 ± 4 μs at 40 psi. All of these reaction times are the same as those obtained for aMb at the same backing pressures. These results indicate that the reaction times obtained using rapid mixing from theta-glass emitters are independent of the different folding time constants for these two proteins, and any uncertainties in the protein folding time constants do not contribute substantially to uncertainties in the reaction times measured here. A reaction time of 7 ± 3 μs was reported[23] from cyt c folding using the same tip size and backing pressure as that used to obtain the 9 ± 2 μs reaction time reported here. A significantly more concentrated aqueous ammonium acetate solution (500 mM) was used in the earlier study compared to the 100 mM aqueous ammonium acetate solution used here. The similar reaction times indicate that the initial concentration of ammonium acetate in the droplets has no measurable effect on the measured reaction times within this range of concentrations.

Reaction Times and Tip Size. Reducing the o.d. of the tips of the theta-glass emitters results in lower flow rates, smaller initial droplet sizes,[39] and shorter droplet lifetimes. The data in Figure 2 were acquired using ~1465 nm o.d. tips. A nanoESI mass spectrum of the acidified aqueous aMb solution (pH = 2.9) acquired using a theta-glass emitter with a significantly smaller ~305 nm o.d. tip is shown in Figure 3, panel a. The charge-state distribution is bimodal, with one distribution between the 12−21+ charge states and the other between the 22−27+ charge states, which comprise 18 ± 3% of the population. The distribution between the 12−21+ charge states is significantly narrower than the distribution corresponding to unfolded conformers (11−26+) obtained with the larger ~1465 nm o.d. tips (Figure 2a). This is possibly a result of a narrower distribution of droplet sizes being formed from the smaller tips. Narrower charge-state distributions have also been reported for cyt c and ubiquitin ions generated from <100 nm o.d. tips compared to those generated from ~1 μm o.d. tips.[51] The 22−27+ charge states observed here may correspond to an even more highly unfolded conformer. Smaller tips have a higher surface area relative to the solution volume, and the surface may cause some changes to the protein conformation prior to droplet formation. Similar results are obtained when either a single barrel or both barrels of the theta-glass emitters are used, indicating that

DOI: 10.1021/jacs.5b13081
J. Am. Chem. Soc. 2016, 138, 3453−3460

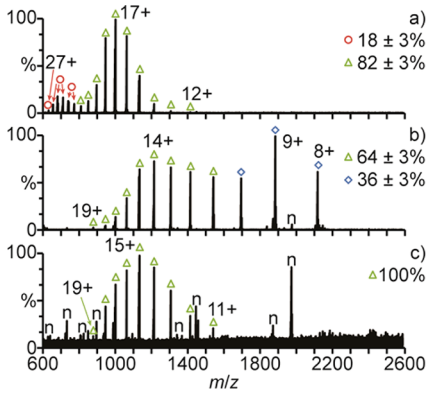

Figure 3. Mass spectra of (a) an acidified aqueous aMb solution (pH = 2.9) and the acidified aMb solution mixed with a 100 mM aqueous ammonium acetate solution (b) at a 1:1 ratio prior to nanoESI (equilibrium; pH = 4.7) and (c) using the theta-glass emitters. (n) denotes noise. All data were acquired using ~305 nm o.d. tips.

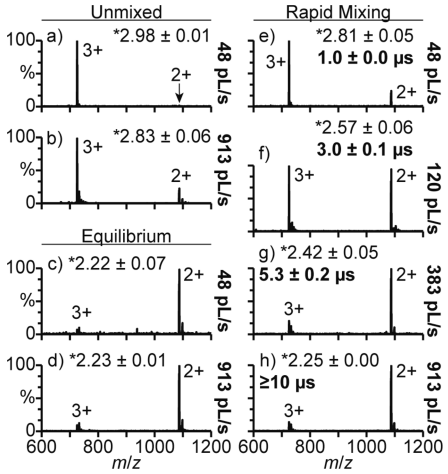

Figure 4. Mass spectra of (a,b) an acidified aqueous Trp-cage solution (pH = 3.4) and (c,d) the acidified Trp-cage solution mixed with a 100 mM aqueous ammonium acetate solution at a 1:1 ratio prior to nanoESI (equilibrium; pH = 5.7) acquired using (a,c) ~244 and (b,d) ~1465 nm o.d. tips. Mass spectra of the acidified Trp-cage solution mixed with the ammonium acetate solution using the theta-glass emitters at flow rates of (e) 48, (f) 120, (g) 383, and (h) 913 pL/s. (*) denotes average charge state.

this distribution is not a result of different droplet size distributions being formed from the different barrels of the theta-glass emitters. The relative abundance of this distribution remains nominally constant when the spray potential is varied between −450 and −1050 V, indicating that this distribution does not result from the increased electric field resulting from the smaller tip size. Charging of protein and peptide ions formed by nanoESI from methanol/water/acid solutions in which proteins are denatured also increases with decreasing tip size.[30,51] This was attributed to the smaller droplets having high charge densities. However, formation of high charge density droplets would not likely result in the bimodal charge state distributions observed here.

Results obtained for the acidified aMb solution mixed with the 100 mM aqueous ammonium acetate solution at a 1:1 ratio prior to nanoESI acquired using a ~305 nm o.d. tip are shown in Figure 3, panel b. Charge states corresponding to folded (8−10+) and unfolded (11−19+) conformers are present, and the folded conformer comprises 36 ± 3% of aMb. There is not a charge-state distribution corresponding to a highly unfolded structure, suggesting that if this structure exists, it is not stable at pH = 4.7. The 8−10+ and 11−19+ charge-state distributions are narrower than those corresponding to the folded (7−10+) and unfolded (11−23+) conformers formed with the ~1465 nm o.d. tips (Figure 2b), consistent with the charge-state distribution narrowing observed for the acidified aMb solution in Figure 3, panel a. The acidified aMb solution and the aqueous ammonium acetate solution were mixed using theta-glass emitters with ~305 nm o.d. tips (Figure 3c), but no charge states corresponding to folded structures were apparent given the low signal-to-noise ratio. On the basis of the noise level, an upper limit to the reaction time of 2.8 ± 0.6 μs is established.

To more effectively measure reaction times when using the small tip sizes, a protein that has a shorter folding time constant than that of the initial collapse of aMb (7 μs) was used. Trp-cage folds from an open structure to a globular loop structure with a 4.1 μs folding time constant at 22.7 °C.[7] Mass spectra of an acidified aqueous Trp-cage solution (pH = 3.4) obtained using theta-glass emitters with ~244 and ~1465 nm o.d. tips are shown in Figure 4, panels a and b, respectively. Both the 2+ and 3+ charge states are formed, and the 3+ is the most abundant in both spectra, though the average charge state is higher from the ~244 nm tips (2.98 ± 0.01, Figure 4a) than from the ~1465 nm tips (2.83 ± 0.06, Figure 4b). This result is consistent with the narrower charge-state distributions observed for aMb conformers when using the smaller tips. Results acquired for the acidified Trp-cage solution mixed with a 100 mM aqueous ammonium acetate solution at a 1:1 ratio prior to nanoESI (equilibrium; pH = 5.7) using ~244 and ~1465 nm o.d. tips are shown in Figure 4, panels c and d, respectively. The 2+ charge state is most abundant, consistent with a change from an unfolded to a folded structure in solution, and the average charge state of Trp-cage is the same to within error for each tip size (2.22 ± 0.07 and 2.23 ± 0.02 in Figure 4c,d, respectively).

The acidified Trp-cage solution was mixed with the ammonium acetate solution using the theta-glass emitters at flow rates of 48−913 pL/s. These flow rates were obtained using various tip sizes and backing pressures. Results from these experiments are shown in Figure 4, panels e−h in order of increasing flow rate. The average charge state decreases with increasing flow rate from 2.81 ± 0.05 at 48 pL/s to 2.25 ± 0.00 at 913 pL/s. These results indicate that the extent of folding occurring in these experiments increases with increasing flow rate. Because the charge state distribution is not bimodal, reaction times for these experiments are obtained from the average charge states (instead of the folded fractions of the protein) using eq 2:

$$t = \tau \ln\left(\frac{q_e - q_o}{q_e - q_t}\right) \quad (2)$$

which is derived from eq 1 by substituting the average charge states at equilibrium and times 0 and t (q_e, q_o, and q_t, respectively) for the relative abundances of the folded protein conformer at these times. Reaction times obtained using eq 2 and the 4.1 μs folding time constant of Trp-cage are indicated on the corresponding mass spectra (Figure 4e−h). The reaction time increases with increasing flow rate from 1.01 ± 0.04 μs at 48 pL/s to 5.3 ± 0.2 μs at 383 pL/s. The 1.0 μs reaction time is significantly less than the shortest reaction time (8 μs) reported for a conventional mixer.[2] This 1.0 μs reaction time is obtained

DOI: 10.1021/jacs.5b13081
J. Am. Chem. Soc. 2016, 138, 3453−3460

using a 48 pL/s flow rate, which is ~2000-times less than the ~100 nL/s flow rate used to obtain the 8 μs reaction time using a conventional mixer. This reaction time is also more than an order of magnitude less than the shortest reaction time (>13 μs) reported for a time resolvable mixing experiment coupled with MS[20] and more than two orders of magnitude less than that for a conventional mixer (200 μs) coupled with MS.[3] At a flow rate of 383 pL/s, a reaction time of 5.3 μs is obtained, which is essentially the same as the 5 ± 2 and 5.5 ± 0.9 μs reaction times obtained for aMb and cyt *c*, respectively, using this same flow rate. This result indicates that the average charge state can be used to monitor protein folding in cases where bimodal charge-state distributions are not produced. At 913 pL/s, the folding of Trp-cage reaches equilibrium during nanoESI. Results from laser-induced temperature-jump experiments indicate that Trp-cage folding reaches equilibrium in about 9−10 μs at 25 °C.[7] This result suggests a lower limit of about 9−10 μs for the reaction time at 913 pL/s, consistent with the 9 ± 2 μs reaction time obtained for both aMb and cyt *c* using this same flow rate. The 9−10 μs equilibration time for Trp-cage folding indicates that this reaction would be near equilibrium within the 8 μs reaction time reported for a conventional mixer, but results reported here illustrate that this fast folding reaction can be readily investigated with mass spectrometry using rapid mixing from theta-glass emitters.

Kinetics of a β-hairpin Formation. β-hairpin formation can occur quickly. The formation of the β-hairpin structure of a 16 residue peptide (protein G B1, fragment 41−56) at room temperature, measured using nanosecond laser temperature-jump experiments, occurs with a time constant of 6 μs.[52] Folding time constants between 0.8 and 20 μs have been estimated for the formation of similar structures for three different 15−17 residue peptides based on computer simulations.[53] To determine if the formation of a β-hairpin structure can be monitored using rapid mixing from theta-glass emitters, the folding of renin substrate tetradecapeptide (RST) was investigated. RST is a 14 residue peptide that adopts a β-hairpin structure in aqueous solutions between pH = 4.0 and 6.0 and is unfolded between pH = 2.5 and 3.6.[54] The rate at which RST folds from an unfolded structure to the β-hairpin structure has not been previously measured. To measure this rate, acid denatured RST is mixed with aqueous ammonium acetate to induce folding using the theta-glass emitters at various reaction times. Mass spectra of an acidified aqueous RST solution (pH = 2.9) obtained using theta-glass emitters with ~244 and ~1465 nm o.d. tips are shown in Figure 5, panels a and b, respectively. Only the 3+ charge state is formed when the smaller ~244 nm tips are used (Figure 5a), but the 2+ charge state is also present at low abundance with the larger ~1465 nm tips (Figure 5b, average charge state =2.89 ± 0.03). These results are consistent with the narrower charge state distributions observed for aMb and Trp-cage conformers when the smaller tips are used. Results from mixing the acidified RST solution with a 100 mM aqueous ammonium acetate solution at a 1:1 ratio prior to nanoESI (equilibrium; pH = 4.7) obtained using ~244 and ~1465 nm o.d. tips are shown in Figure 5, panels c and d, respectively. The 2+ charge state is predominantly formed (>93% of RST), resulting in an average charge state of 2.06 ± 0.00 and 2.04 ± 0.01 for the ~244 and ~1465 nm o.d. tips, respectively. The change in charge state from predominantly a 3+ (Figure 5a,b) to predominantly a 2+ (Figure 5c,d) is consistent with a change from an unfolded to a folded structure in solution.

Results from mixing the acidified RST solution with the ammonium acetate solution using the theta-glass emitters with flow rates that result in reaction times of between 1.0 and 9.1 μs

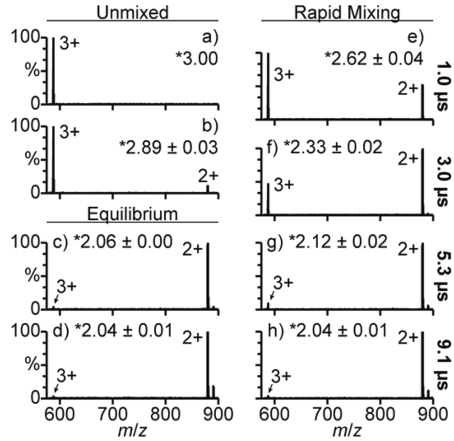

Figure 5. Mass spectra of (a,b) an acidified aqueous RST solution (pH = 2.9) and (c,d) the acidified RST solution mixed with a 100 mM aqueous ammonium acetate solution at a 1:1 ratio prior to nanoESI (equilibrium; pH = 4.7) acquired using (a,c) ~244 and (b,d) ~1465 nm o.d. tips. Mass spectra of the acidified RST solution mixed with the ammonium acetate solution using the theta-glass emitters with flow rates that result in reaction times of (e) 1.0, (f) 3.0, (g) 5.3, and (h) 9.1 μs. (∗) denotes average charge state.

(average of values obtained for aMb, cyt *c*, and Trp-cage) are shown in Figure 5, panels e−h in order of increasing reaction time. The average charge state decreases with increasing reaction time from 2.62 ± 0.04 at 1.0 μs to 2.04 ± 0.01 at 9.1 μs. For reaction times of 1.0−5.3 μs (Figures 5e−g), the average charge state of RST is higher than that resulting from the premixed solution at equilibrium (Figure 5c,d), but at 9.1 μs (Figure 5h), the average charge state is the same as that resulting from the premixed solution at equilibrium. These results indicate that the folding of RST does not reach equilibrium within ≤5.3 μs but does reach equilibrium within 9.1 μs. The folding time constant for the formation of the β-hairpin structure is obtained from the rapid mixing data at short times (Figure 5e−g) using eq 2. Folding time constants of 2.0 ± 0.3, 2.3 ± 0.2, and 2.2 ± 0.2 μs are obtained at reaction times of 1.0, 3.0, and 5.3 μs, respectively. These values are the same to within error, and the average value is 2.2 ± 0.3 μs. These results indicate that RST folds from an unfolded structure to a β-hairpin structure within a few μs. To the best of our knowledge, this is the fastest folding event that has been directly monitored using a rapid mixing technique. These results indicate that fast folding events that occur on the low μs time scale can be readily investigated using rapid mixing from theta-glass emitters with mass spectrometry detection.

Reaction Temperature. Protein conformation and folding time constants depend on temperature.[7,41] Temperature regulated ESI capillaries have been used to measure the thermal stabilities of folded forms of proteins at equilibrium[34,55−58] as well as to investigate protein complexation[59] and aggregation[57] as a function of temperature. Thermal unfolding midpoint temperatures and association constants have been obtained using temperature regulated ESI capillaries that are the same as those obtained using traditional solution-phase techniques such as fluorescence spectroscopy,[55,56] isothermal titration calorimetry,[59] and differential scanning calorimetry.[57] These results suggest that the temperature of the ESI droplets reflects that of the original solution. To obtain information about the droplet temperature in our rapid mixing experiments, the fraction of Trp-cage that is unfolded as a function of temperature was measured using temperature regulated ESI capillaries.[34] Mass spectra of the

DOI: 10.1021/jacs.5b13081
J. Am. Chem. Soc. 2016, 138, 3453−3460

acidified Trp-cage solution mixed with the ammonium acetate solution at a 1:1 ratio prior to nanoESI (equilibrium; pH = 5.7) acquired at capillary temperatures of 25, 45, and 65 °C are shown in Figure 6, panel a. The relative abundance of the 3+ charge state

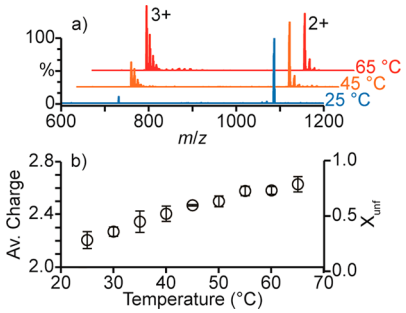

Figure 6. (a) Mass spectra of an acidified aqueous Trp-cage solution mixed with a 100 mM aqueous ammonium acetate solution at a 1:1 ratio prior to nanoESI (equilibrium, pH = 5.7) acquired at capillary temperatures of 25 (blue), 45 (orange), and 65 (red) °C. (b) The average charge state (left axis) and fraction unfolded (X_{unf}, right axis) of Trp-cage resulting from this solution as a function of the capillary temperature.

increases with increasing solution temperature, consistent with thermal denaturation of Trp-cage in solution prior to nanoESI.

The relative ion abundances in a bimodal charge-state distribution directly reflect the populations of folded and unfolded structures. In cases where a bimodal charge-state distribution is not formed, information about folding is deduced from changes in the average charge state, but the abundances of the folded and unfolded populations are not obtained. The charge-state distribution of Trp-cage is not bimodal. Thus, it is not possible to obtain the abundances of the folded and unfolded forms of Trp-cage from these temperature-dependent experiments alone. This information can be obtained from the average charge state by comparing our results to those measured in solution using more conventional structural methods. The fraction of Trp-cage that is unfolded at 25 °C is 28% in aqueous buffer solutions.[7] If the solution temperature and the droplet temperature are similar, our results measured at 25 °C (Figure 6a) indicate that a 28% unfolded population corresponds to an average charge state of 2.21 ± 0.06. If Trp-cage is fully unfolded at pH = 3.4, then the fully unfolded form has an average charge state of 2.83 ± 0.06 (Figure 4b). Assuming that the average charge state is a linear superposition of the charge states corresponding to the folded and unfolded conformers, the temperature dependent charge-state distributions in Figure 6, panel a can be used to obtain the relative abundances of these two conformers in these experiments. The average charge state (left axis) and the resulting fraction unfolded (right axis) of Trp-cage as a function of temperature are shown in Figure 6, panel b. The fraction of Trp-cage that is unfolded increases from 34% at 30 °C to 77% at 65 °C. The fraction of Trp-cage that is unfolded at 30 and 65 °C measured in solution previously is 35% and 80%, respectively.[7] All of the data measured in solution[7] and the data obtained using the average charge states reported here are the same to within 4% over this temperature range. The Trp-cage data were obtained using a flow rate that results in a 9.1 μs reaction time. Thus, Trp-cage could fold or unfold if the droplet temperature was significantly lower or higher, respectively, than the initial solution temperature. The close agreement between the extent of unfolding observed in our temperature-dependent theta-glass emitter experiments and those measured in solution using conventional structural methods indicates that the droplet temperature is similar to the temperature of the initial solution and that any changes in the droplet temperature that may occur do not significantly affect folding time constants measured using our rapid mixing technique at room temperature.

CONCLUSIONS

Rapid mixing of two solutions to measure reaction times as short as 1.0 μs is demonstrated using theta-glass emitters combined with MS detection. Reaction times were measured by monitoring the pH induced folding of three proteins with folding time constants ranging from 4.1−57 μs. The extent of folding that occurs in these experiments depends on the initial droplet size, which was controlled by varying the solution flow rate from 48−2880 pL/s, resulting in reaction times of between 1.0 and 22 μs. The reaction times obtained for all three proteins at the same flow rates are nearly identical, indicating that reaction times can be accurately obtained from these protein folding measurements. These reaction times are upper limits to the lifetimes of the ESI droplets because some product formation likely occurs in the Taylor cone prior to droplet formation.[21,22] The shortest reaction time (1 μs) achieved in these experiments is significantly shorter than that achieved using conventional mixers (8 μs).[2] This 1.0 μs reaction time is obtained using a 48 pL/s flow rate, which is 2000-fold less than the flow rate used to obtain the 8 μs reaction time using a conventional mixer (~100 nL/s), demonstrating that substantially less sample is required to perform these fast mixing experiments.

A folding time constant of 2.2 μs for the formation of the β-hairpin structure of RST was measured using rapid mixing with theta-glass emitters. This is the fastest folding event that has been directly monitored using a rapid mixing technique. Results from this experiment demonstrate that fast folding events that occur in as fast as a few microseconds can be readily investigated using rapid mixing from theta-glass emitters. Rapid mixing from theta-glass emitters also has the advantage of high chemical specificity and sensitivity provided by the MS detection, which should make it possible to measure complex reactions with multiple reaction products. This capability should make these devices generally applicable to measuring kinetic parameters for a diverse range of fast reactions. By using unimolecular reaction processes, such as protein folding, to establish reaction times at different flow rates, quantitative information about enhanced reaction rates for bimolecular or more complex reactions as a result of droplet evaporation[60] and droplet surface effects could be obtained.

ASSOCIATED CONTENT

Supporting Information

The Supporting Information is available free of charge on the ACS Publications website at DOI: 10.1021/jacs.5b13081.

Electron micrographs of the tips of the theta-glass emitters, mixing efficiency measurements obtained using the complexation reaction between K^+ and 18C6, and TWIMS drift profiles obtained for the folded forms of aMb and cyt *c* resulting from equilibrium and rapid mixing experiments (PDF)

AUTHOR INFORMATION

Corresponding Author

*erw@berkeley.edu

DOI: 10.1021/jacs.5b13081
J. Am. Chem. Soc. 2016, 138, 3453−3460

Notes

The authors declare no competing financial interest.

■ ACKNOWLEDGMENTS

The authors thank Zijie Xia for helpful discussion, the Robert D. Ogg Electron Microscope Lab at the University of California, Berkeley for use of the Hitachi TM-1000 scanning electron microscope, and the National Institutes of Health for funding (R01GM097357).

■ REFERENCES

(1) Kolakowski, B.; Konermann, L. *Anal. Biochem.* **2001**, *292*, 107−114.
(2) Wu, L.; Lapidus, L. J. *Anal. Chem.* **2013**, *85*, 4920−4924.
(3) Vahidi, S.; Stocks, B. B.; Liaghati-Mobarhan, Y.; Konermann, L. *Anal. Chem.* **2013**, *85*, 8618−8625.
(4) Zinck, N.; Stark, A.; Wilson, D. J.; Sharon, M. *ChemistryOpen* **2014**, *3*, 109−114.
(5) Li, Y.; Zhang, D.; Feng, X.; Xu, Y.; Liu, B. *Talanta* **2012**, *88*, 175−180.
(6) Matsumoto, S.; Yane, A.; Nakashima, S.; Hashida, M.; Fujita, M.; Goto, Y.; Takahashi, S. *J. Am. Chem. Soc.* **2007**, *129*, 3840−3841.
(7) Qiu, L.; Pabit, S.; Roitberg, A.; Hagen, S. *J. Am. Chem. Soc.* **2002**, *124*, 12952−12953.
(8) Lee, E. D.; Muck, W.; Henion, J. D.; Covey, T. R. *J. Am. Chem. Soc.* **1989**, *111*, 4600−4604.
(9) Simmons, D. A.; Konermann, L. *Biochemistry* **2002**, *41*, 1906−1914.
(10) Hong, C.; Tsai, F.; Shiea, J. *Anal. Chem.* **2000**, *72*, 1175−1178.
(11) Shiea, J.; Chang, D.; Lin, C.; Jiang, S. *Anal. Chem.* **2001**, *73*, 4983−4987.
(12) Shieh, I.; Lee, C.; Shiea, J. *J. Proteome Res.* **2005**, *4*, 606−612.
(13) Chen, H.; Venter, A.; Cooks, R. G. *Chem. Commun.* **2006**, *19*, 2042−2044.
(14) Tian, Y.; Chen, J.; Ouyang, Y.; Qu, G.; Liu, A.; Wang, X.; Liu, C.; Shi, J.; Chen, H.; Jiang, G. *Anal. Chim. Acta* **2014**, *814*, 49−54.
(15) Prudent, M.; Rossier, J. S.; Lion, N.; Girault, H. H. *Anal. Chem.* **2008**, *80*, 2531−2538.
(16) Miladinovic, S. M.; Fornelli, L.; Lu, Y.; Piech, K. M.; Girault, H. H.; Tsybin, Y. O. *Anal. Chem.* **2012**, *84*, 4647−4651.
(17) Girod, M.; Moyano, E.; Campbell, D. I.; Cooks, R. G. *Chem. Sci.* **2011**, *2*, 501−510.
(18) Miao, Z.; Chen, H.; Liu, P.; Liu, Y. *Anal. Chem.* **2011**, *83*, 3994−3997.
(19) Badu-Tawiah, A. K.; Campbell, D. I.; Cooks, R. G. *J. Am. Soc. Mass Spectrom.* **2012**, *23*, 1077−1094.
(20) Lee, J. K.; Kim, S.; Nam, H. G.; Zare, R. N. *Proc. Natl. Acad. Sci. U. S. A.* **2015**, *112*, 3898−3903.
(21) Mortensen, D. N.; Williams, E. R. *Anal. Chem.* **2014**, *86*, 9315−9321.
(22) Mark, L. P.; Gill, M. C.; Mahut, M.; Derrick, P. J. *Eur. J. Mass Spectrom.* **2012**, *18*, 439−446.
(23) Mortensen, D. N.; Williams, E. R. *Anal. Chem.* **2015**, *87*, 1281−1287.
(24) Fisher, C. M.; Kharlamova, A.; McLuckey, S. A. *Anal. Chem.* **2014**, *86*, 4581−4588.
(25) Grimm, R. L.; Beauchamp, J. L. *Anal. Chem.* **2002**, *74*, 6291−6297.
(26) Pfeifer, R. J.; Hendricks, C. D., Jr. *AIAA J.* **1968**, *6*, 496−502.
(27) De La Mora, J. F.; Loscertales, I. G. *J. Fluid Mech.* **1994**, *260*, 155−184.
(28) Wilm, M. S.; Mann, M. *Int. J. Mass Spectrom. Ion Processes* **1994**, *136*, 167−180.
(29) Tang, K.; Gomez, A. *J. Colloid Interface Sci.* **1996**, *184*, 500−511.
(30) Li, Y.; Cole, R. B. *Anal. Chem.* **2003**, *75*, 5739−5746.
(31) Mirza, U.; Cohen, S.; Chait, B. *Anal. Chem.* **1993**, *65*, 1−6.
(32) Kaltashov, I.; Eyles, S. *Mass Spectrom. Rev.* **2002**, *21*, 37−71.
(33) Liu, J.; Konermann, L. *J. Am. Soc. Mass Spectrom.* **2009**, *20*, 819−828.
(34) Sterling, H. J.; Williams, E. R. *J. Am. Soc. Mass Spectrom.* **2009**, *20*, 1933−1943.
(35) Konermann, L.; Rosell, F. I.; Mauk, A. G.; Douglas, D. J. *Biochemistry* **1997**, *36*, 6448−6454.
(36) Jurchen, J. C.; Williams, E. R. *J. Am. Chem. Soc.* **2003**, *125*, 2817−2826.
(37) Blakney, G. T.; Hendrickson, C. L.; Marshall, A. G. *Int. J. Mass Spectrom.* **2011**, *306*, 246−252.
(38) *CRC Handbook of Chemistry and Physics*, 55th ed.; Weast, R. C., Ed.; CRC Press: Boca Raton, FL, 1974.
(39) Schmidt, A.; Karas, M.; Dülcks, T. *J. Am. Soc. Mass Spectrom.* **2003**, *14*, 492−500.
(40) Goto, Y.; Fink, A. L. *J. Mol. Biol.* **1990**, *214*, 803−805.
(41) Gilmanshin, R.; Callender, R.; Dyer, R. *Nat. Struct. Biol.* **1998**, *5*, 363−365.
(42) Ballew, R.; Sabelko, J.; Gruebele, M. *Proc. Natl. Acad. Sci. U. S. A.* **1996**, *93*, 5759−5764.
(43) Callender, R.; Dyer, R.; Gilmanshin, R.; Woodruff, W. *Annu. Rev. Phys. Chem.* **1998**, *49*, 173−202.
(44) Shastry, R. M. C.; Luck, S. D.; Roder, H. *Biophys. J.* **1998**, *74*, 2714−2721.
(45) Konno, T. *Protein Sci.* **1998**, *7*, 975−982.
(46) Stellwagen, E.; Babul, J. *Biochemistry* **1975**, *14*, 5135−5140.
(47) Krantz, B.; Mayne, L.; Rumbley, J.; Englander, S.; Sosnick, T. *J. Mol. Biol.* **2002**, *324*, 359−371.
(48) Kathuria, S. V.; Chan, A.; Graceffa, R.; Nobrega, R. P.; Matthews, C. R.; Irving, T. C.; Perot, B.; Bilsel, O. *Biopolymers* **2013**, *99*, 888−896.
(49) Takahashi, S.; Yeh, S.; Das, T.; Chan, C.; Gottfried, D.; Rousseau, D. *Nat. Struct. Biol.* **1997**, *4*, 44−50.
(50) Chan, C.; Hu, Y.; Takahashi, S.; Rousseau, D.; Eaton, W.; Hofrichter, J. *Proc. Natl. Acad. Sci. U. S. A.* **1997**, *94*, 1779−1784.
(51) Yuill, E. M.; Sa, N.; Ray, S. J.; Hieftje, G. M.; Baker, L. A. *Anal. Chem.* **2013**, *85*, 8498−8502.
(52) Munoz, V.; Thompson, P. A.; Hofrichter, J.; Eaton, W. A. *Nature* **1997**, *390*, 196−199.
(53) Kubelka, J.; Hofrichter, J.; Eaton, W. A. *Curr. Opin. Struct. Biol.* **2004**, *14*, 76−88.
(54) Oliveira, M. C. F.; Juliano, L.; Paiva, A. C. M. *Biochemistry* **1977**, *16*, 2606−2611.
(55) Benesch, J.; Sobott, F.; Robinson, C. *Anal. Chem.* **2003**, *75*, 2208−2214.
(56) Geels, R. B. J.; Calmat, S.; Heck, A. J. R.; van der Vies, S. M.; Heeren, R. M. A. *Rapid Commun. Mass Spectrom.* **2008**, *22*, 3633−3641.
(57) Wang, G.; Abzalimov, R. R.; Kaltashov, I. A. *Anal. Chem.* **2011**, *83*, 2870−2876.
(58) Chen, L. C.; Rahman, M. M.; Hiraoka, K. *J. Am. Soc. Mass Spectrom.* **2014**, *25*, 1862−1869.
(59) Daneshfar, R.; Kitova, E. N.; Klassen, J. S. *J. Am. Chem. Soc.* **2004**, *126*, 4786−4787.
(60) Badu-Tawiah, A. K.; Campbell, D. I.; Cooks, R. G. *J. Am. Soc. Mass Spectrom.* **2012**, *23*, 1461−1468.

DOI: 10.1021/jacs.5b13081
J. Am. Chem. Soc. 2016, 138, 3453−3460